Environmental Pollution 324 (2023) 121375

Contents lists available at ScienceDirect

Environmental Pollution

journal homepage: www.elsevier.com/locate/envpol

# Low dosage fluorine ameliorates the bioaccumulation, hepatorenal dysfunction and oxidative stress, and gut microbiota perturbation of cadmium in rats☆

Dashuan Li [a,1], Chaolian Yang [a,1], Xiaomei Xu [a], Shanghang Li [a], Guofei Luo [a], Cheng Zhang [a], Zelan Wang [a], Dali Sun [a], Jianzhong Cheng [b], Qinghai Zhang [a,*]

[a] School of Public Health /the Key Laboratory of Environmental Pollution Monitoring and Disease Control, Ministry of Education, Guizhou Medical University, Guiyang, 550025, China

[b] State Key Laboratory of Environmental Geochemistry, Institute of Geochemistry, Chinese Academy of Sciences, Guiyang, 550081, China

ARTICLE INFO

*Keywords:*
Cd
F
Accumulation
Hepatorenal function injuries
Hepatorenal oxidative stress
Intestinal microflora disorders

ABSTRACT

Many "hot spot" geographic areas around the world with soils and crops co-polluted with cadmium (Cd) and fluorine (F), two of the most representative pollutants in the environment. However, it still exists argumentative on the dose-effect relationship between F and Cd so far. To explore this, a rat model was established to evaluate the effects of F on Cd-mediated bioaccumulation, hepatorenal dysfunction and oxidative stress, and the disorder of intestinal microbiota as well. 30 healthy rats were randomly assigned to Control group (C group), Cd 1 mg/kg (Cd group), Cd 1 mg/kg and F 15 mg/kg (L group), Cd 1 mg/kg and F 45 mg/kg (M group), and Cd 1 mg/kg and F 75 mg/kg (H group) for 12 weeks by gavage. Our results showed that Cd exposure could accumulate in organs, cause hepatorenal function damage and oxidative stress, and disorder of gut microflora. However, different dosages of F showed various effects on Cd-induced damages in liver, kidney, and intestine, and only the low supplement of F showed a consistent trend. After low supplement of F, Cd levels were declined by 31.29% for liver, 18.31% for kidney, and 2.89% for colon, respectively. The serum aspartate aminotransferase (AST), blood urea nitrogen (BUN), creatinine (Cr), and N-acetyl-β-glucosaminidase (NAG) were significantly reduced ($p < 0.01$); The activity of superoxide dismutase (SOD) was elevated and mRNA expression level of NAD(P)H quinone oxidoreductase 1 (*NQO1*) was decreased in the liver and kidney ($p < 0.05$). Moreover, low F dosage up-regulated the abundance of *Lactobacillus* from 15.56% to 28.73% and the 6.23% of F/B ratio was declined to 3.70%. Collectively, this highlights that low dosage of F might be a potential strategy to ameliorate the hazardous effects by Cd-exposed in the environment.

## 1. Introduction

Cadmium (Cd) and fluorine (F) have been recognized as hazardous contaminants to threaten food security and aroused public concerns extensively (Duan et al., 2021). Cd is one of the Group I human carcinogen element that injure the human health with a long half-life of 10–30 years (Wang et al., 2023). The scientific data reported that its exposure is harmful to approximately 10% population around the world with a higher mortality rate (Bhardwaj et al., 2021). F is ubiquitous in the environment, which is propitious for dental caries prevention at certain dosages (Yu et al., 2021). However, high levels of F can elevate F absorption in the body by the digestive tract (Yu et al., 2021). It is reported that about more than 200 million persons are suffered from exceeding 1.5 mg/L fluoride risk worldwide (Han et al., 2019). F and Cd can react to form $CdF^{+}$ complexes when pH > 6.3 in the environment, which is more easily taken up by crops and bioaccumulated in animals and humans (Yu and Yang, 2020). Many "hot spot" geographic areas around the world were observed co-polluted by the F and Cd (Li et al., 2019). Previously, our group had investigated the concentrations of F

☆ This paper has been recommended for acceptance by Mingliang Fang.

* Corresponding author.

*E-mail addresses:* lidashuan1997@163.com (D. Li), yangcl414@163.com (C. Yang), xxm5209960807@163.com (X. Xu), lsh961221@163.com (S. Li), LGUOFEI2022@163.com (G. Luo), Chengz76@gmc.edu.cn (C. Zhang), wzl2010kaoyun@163.com (Z. Wang), dalisun11@163.com (D. Sun), chengjianzhong@vip.gyig.ac.cn (J. Cheng), zhqh@gmc.edu.cn (Q. Zhang).

[1] Dashuan Li and [1]Chaolian Yang contributed equally to this work and share the first authorship.

https://doi.org/10.1016/j.envpol.2023.121375
Received 5 December 2022; Received in revised form 24 February 2023; Accepted 27 February 2023
Available online 28 February 2023

| Abbreviation | Full title |
|---|---|
| ALT | Alanine aminotransferase |
| ANOVA | One-way analysis of variance |
| AREs | Antioxidant response elements |
| AST | Aspartate aminotransferase |
| BUN | Blood urea nitrogen |
| CAT | Catalase |
| Cd | Cadmium |
| Cr | Creatinine |
| F | Fluorine |
| GSH-Px | Glutathione peroxidase |
| H&E | Hematoxylin and eosin |
| HQ1 | Heme oxygenase-1 |
| Keap1 | Kelch-like ECH associating protein 1 |
| MDA | Malondialdehyde |
| NAG | N-acetyl-β-glucosaminidase |
| NQO1 | NAD(P)H quinone oxidoreductase 1 |
| Nrf2 | Nuclear factor erythroid 2-related factor 2 |
| ROS | Reactive oxygen species |
| RT-qPCR | Real-time quantitative polymerase chain reaction |
| SD | Sprague Dawley |
| SOD | Superoxide dismutase |
| TISAB | Total ionic strength adjustment buffer |

and Cd in crops of karst region, finding that co-exposure of F and Cd could pose non-carcinogenic risks to the local populace (Li et al., 2023; Li et al., 2022). Therefore, attention should be paid to the adverse effects of co-exposure of Cd and F to human beings.

Previous studies verified that Cd and F exposed to animals and humans may cause bioaccumulation in liver, kidney, and intestine, thereby constantly producing detrimental impacts on living organisms (Wang et al., 2019; Wang et al., 2020; Xu et al., 2021). Zhang et al. indicated that the activities of superoxide dismutase (SOD), catalase (CAT), and glutathione peroxidase (GSH-Px) are changed with the presence of Cd, suggesting that the organism may appear oxidative damage (Zhang et al., 2017). It can exert nuclear factor erythroid 2-related factor 2 (Nrf2) dissociation from kelch-like ECH associating protein 1 (Keap1), resulting in Nrf2 translocate into the nucleus and binding to antioxidant response elements (AREs) in the promoter regions of target genes to decline the antioxidant capacity (Fan et al., 2020). Furthermore, the evidence confirmed that the F-mediated pathogenesis is happened with the ease of reactive oxygen species (ROS), peroxyl and hydroxyl radical formation, leading to oxidative stress (Alhusaini et al., 2018). Given Cd and F exposure via drinking water, Zhang et al. (2013) showed that serum ALT and urinary β2-microglobulin of rats were statistically higher than that in the non-treated group, indicating hepatorenal function injuries were produced by F and Cd. These discussions above showed that stable toxicities for Cd and F are observed in the liver and kidney, which possibly exerted their toxic effects via triggering oxidative stress and function damage (Gong et al., 2022; Tian et al., 2019; Wang et al., 2022).

Taking the hazardous effect of Cd and F on intestine into consideration as well, the gut microbiota, which exists in symbiosis with gut epithelial cells, could be influenced by these two contaminant exposures. In the presence of Cd, the gut microbiota composition was altered and some bacteria were likely to be developed as biomarkers for certain diseases (Ba et al., 2017). It is reported that Bacteroides, Aeromonas, and Bacillus were significantly altered after Cd exposure (1 mg/L) (Wang et al., 2020). In addition, Liu et al. (2019) showed that excessive F (50 mg/L) greatly shifted the gut microbiota composition in mice. However, Chen et al. (2021b) stressed that the effects of F to gut microbiota depended on its doses. Specifically, low level of F (1 mg/L) could enhance the growth of helpful intestinal microbiota (Faecalibacterium and Lactobacillus), while a high F level (15 mg/L) elevated the hazardous bacterium including Proteobacteria, and Enterobacteriaceae. The aforementioned results evidenced that F or Cd exposure could pose perturbations of intestinal microbiota.

So far, although previous experiments have demonstrated the impacts on the co-exposure of Cd and F to evaluate their relationship, the results are still controversial. Chen et al. (2013) evidenced that low dosage of F (20 mg/L) could reverse the decrease of vertebral bone mineral density by Cd-induced, suggesting that there might be an antagonistic action between F and Cd. However, it is shown that the concurrent F and Cd could promote histopathological injuries and mitochondrial dysfunction compared with F and Cd alone (Milad et al., 2020), indicating that a synergistic reaction was observed between F and Cd. Therefore, it is still scarce whether co-exposure of Cd and F causes synergistic or antagonistic reactions and the underlying molecular mechanisms need to be elucidated. To this end, considering that F is beneficial for body growth at a certain level and has a favorable binding property to Cd, our team proposes a scientific hypothesis that whether the two-side effect of co-exposure to F and Cd is determined by the different dosages of F?

To explore this, a rat model by gavage was established to estimate the effects of different F dosages on Cd-mediated bioaccumulation, hepatorenal function damage and oxidative stress, as well as the disorder of the intestinal microbiota. As a beneficial attempt, the present study can be helpful for clarifying the dose-effect relationship of F and Cd and is the first to explore the possibility of different dosages of F ameliorating Cd toxicity, which would provide a novel and significant perspective into alleviating Cd and F toxicity.

## 2. Materials and methods

### 2.1. Chemicals

Cadmium chloride ($CdCl_2{\cdot}2.5H_2O$) with 99.0% and Sodium fluoride (NaF) with 99.5% were purchased from the Tianjin Kemiou Co., Ltd, China. Other chemicals and reagents applied in the experiment all belonged to analytical grade.

### 2.2. Animal experimentation and sample acquisition

Thirty healthy Sprague-Dawley (SD) male rats (220 ± 20 g) were purchased from Liaoning Changsheng Biotechnology Co., Ltd (License No. SCXK (Liao)) 2020–0001, China) and passed the ethical review of Animal Research of Guizhou Medical University (1900947). The rats were feed adaptively for seven days and stochastically assigned into 5 groups (6 rats per group): Control group (C group), Cd 1 mg/kg (Cd group), Cd 1 mg/kg and F 15 mg/kg (L group), Cd 1 mg/kg and F 45 mg/kg (M group), and Cd 1 mg/kg and F 75 mg/kg (H group) and treated through gavage. Among them $CdCl_2{\cdot}2.5H_2O$ and NaF were dissolved and diluted with ultrapure water. The grouped concentrations are set and converted on the basis of previous literature (Nair et al., 2015) and approximate intake level in agricultural products of Guizhou province, China (Data were not published). During cultivation, all rats were housed in the SPF laboratory under the environmental conditions (22 ± 5 °C, 55 ± 1%) with 12 h dark/light cycle, and standard diet and water were accessible freely.

After three months of rearing, all of rats were fasted for one day and water drinking was allowed. All rats were euthanized by injecting pentobarbital. Whole samples of blood were gathered by cardiac puncture through the diaphragm and, then isolated in the serum at 4 °C (3000 rpm, 5 min) for biochemical assessment. Meanwhile, the liver,

kidney, and colon tissues were excised immediately and washed using pre-cooled physiological saline. Each sample was cut as 30 cubic millimeters and placed in 10% formalin for pathological measurements. The rest was stored at −80 °C until further detected.

### 2.3. Determination of Cd and F levels

After weighing, the liver, kidney, and colon samples were acid-digested by 5 mL of concentrated nitric acid (95% $HNO_3$) for 4 h at 140 °C until solution became colorless and transparent, and then liquid was diluted to 10 mL by adding ultrapure water. Thereafter, Cd levels were measured by an inductively coupled plasma mass spectrometry (NexION 2000 ICP-MS, PerkinElmer, USA) as previously published by Tian et al. (2021). The potentiometric method was conducted to examine F level using a fluoride selective ion electrode (Orion, Thermo Scientific, Massachusetts, USA) (Quadri et al., 2018). Liver, kidney, and colon tissues were diluted and determined in total ionic strength adjustment buffer (TISAB) to keep constant ionic strength and remove certain interferences.

### 2.4. Histopathological examination

At room temperature, the liver, kidney, and colon sections were processed with fixing in 4% paraformaldehyde for 24 h. And the prepared sections were dehydrated with certain concentrations of ethanol and cleared with xylene. After embedding in paraffin wax, the tissues were sliced at 5 mm and analyzed by hematoxylin and eosin (H&E) and observed separately under a light microscope (OLYMPUS B-40) (Shi et al., 2023).

### 2.5. Biochemical assays

In order to evaluate the hepatorenal functions, the serum samples were prepared for determination of aspartate aminotransferase (AST), alanine aminotransferase (ALT), alkaline phosphatase (AKP), blood urea nitrogen (BUN), creatinine (Cr), and urine N-acetyl-β-glucosaminidase (NAG). The liver, kidney, and colon tissues were washed and weighted for homogenates in cold normal saline and centrifugation at 3000 rpm and 4 °C for 10 min. Then the superoxide dismutase (SOD), glutathione peroxidase (GSH-Px) activities, and malondialdehyde (MDA) levels were detected. All of biomarkers were measured according to the manufacturer's assay kit from Nanjing Jiancheng Bioengineering, China.

### 2.6. RT-qPCR measurement of gene expression

To analyze the toxic effects of Cd and F, a real-time quantitative polymerase chain reaction (RT-qPCR) analysis was executed (Xu et al., 2022). Total RNA was gathered from kidney, liver, and colon sections with Trizol reagent following the related instruction (Wuhan service bio-Technology Co., Ltd, China). The RNA quality was estimated using OD 260/280 ratio and agarose gel electrophoresis. Then the first-strand complementary DNA (cDNA) was synthesized using the Prime Script Reverse Transcription Reagent kit with gDNA Eraser (Takara, Beijing, China). And the expression levels of antioxidant genes quantified by RT-qPCR were analyzed through TB Green Premix Ex *Taq*II (Takara, Beijing, China). A 20 μL reaction volume using a CFX96 real-time PCR detection system (Bio-Rad, USA) was used to conduct purification initiating at 95 °C for10 min, followed by 40 cycles at 95 °C for 10 s for denaturation, thereafter annealing at 60 °C for 30 s. GAPDH was applied for reference genes to standardize the expression levels of target genes with values shown as $2^{-\Delta\Delta Ct}$ and the primer sequences performed in our research were provided in Table S1 (Shi et al., 2022).

### 2.7. 16 S rDNA gene sequencing and bioinformatics analysis

The total DNA for colon samples was extracted by the CTAB according to the instruction. The V3–V4 hypervariable regions of the bacterial 16 S rDNA gene were amplified by the forward primer 341 F (5′-CCTACGGGNGGCWGCAG-3′) and the reverse primer 806 R 805 R (5′-GACTACHVGGGTATCTAATCC-3′). Amplification of PCR was conducted in a 25 μl reaction mixture containing 25 ng of template DNA, 12.5 μl of PCR premix, 2.5 μl of each primer, and PCR grade water to modulate the volume. The PCR conditions for amplification of the prokaryotic 16s fragment included initial denaturation at 98 °C for 30 s; denaturation at 98 °C for 10 s, annealing at 54 °C for 30 s, extension at 72 °C for 45 s; and finally extension at 72 °C for 10 min. The PCR product was confirmed by 2% agarose gel electrophoresis, which was purified with pure XT beads (Beckman Coulter Genomics, Danforth, USA) and quantified by quantum bit (Invitrogen, USA). Amplicon pools were prepared for sequencing and the size and number of amplicon libraries were evaluated on an Agilent 2100 Bioanalyzer (USA) and Illumina library quantification kit (Kappa Biosciences, Woburn, USA, USA), respectively.

Samples were sequenced on an Illumina NovaSeq platform offered by LC-Bio (Bio Lianchuan Co., Ltd). Alpha and Beta diversities were determined by normalizing to similar sequences. On the basis of SILVA (release 138) classifier, feature abundance was standardized by the relative abundance of every sample. Alpha diversity was used to analyze species diversity for a sample through Chao1, Goods coverage, and Shannon indices. Beta diversity was determined by the method of PCoA. All the statistics were expressed by QIIME2 and the figures were drawn by the R package (v3.5.2).

### 2.8. Statistical analysis

Statistical analysis and graph presentation were executed by IBM SPSS Statistics 22 and GraphPad prism 9.3, and all data was presented as mean ± standard error (mean ± SEM). The statistical differences among groups were calculated by one-way analysis of variance (ANOVA) followed by Tukey's multiple comparisons test with $p \leq 0.05$ being statistically significant.

## 3. Results

### 3.1. F inhibits Cd accumulation in kidney, liver, and colon tissues

To estimate the body distributions of Cd on organs, the accumulation of Cd and F in the liver, kidney, and colon tissues were measured (Table 1). Relative to the Cd group, the accumulations for Cd three parts were decreased significantly by 31.29%, 18.31%, and 2.89% in the L group, 59.66%, 19.25%, and 19.08% in the M group, and 79.70%, 64.39%, and 47.78% in the H group, respectively. It indicated that F treatment markedly ($p < 0.01$) declined the Cd concentration on tissues in a dose-dependent manner. Moreover, the levels of Cd and F in each tissue were in a downward trend of kidney > liver > colon.

### 3.2. Low dosage of F alleviates Cd-induced histopathology damage

The light microscopic observation of liver, kidney, and colon sections in the C group revealed a normal architecture (Fig. 1a1, 1b1 and 1c1). Compared to the C group, Cd treatment caused hepatocyte necrosis in the liver (Fig. 1a2). The dilation of the hepatic sinusoid in the L group was observed (Fig. 1a3). And nuclear solidification accompanied by nuclear fragmentation was observed in the M and H groups (Fig. 1a4 and 1a5). Relative to the C group, the histopathological alterations of the kidney were happened in the renal cortex of the Cd, M, and H groups, including glomerular atrophy, inflammatory reaction, and vitreous degeneration (Fig. 1b2 and 1b5). However, those alterations mentioned above in the L group were lighter than that those groups (Fig. 1b3 and 1b4). Besides, the thickness of the intestine mucosa and glands in the Cd and H groups statistically decreased compared to the C group (Fig. 1c2 and 1c5). However, no obvious evidence reveals the intestine damage in

**Table 1**
Effects of F on the change of Cd levels in organs (mg/kg).

| Group | Cd | | | F | | |
|---|---|---|---|---|---|---|
| | liver | kidney | colon | liver | kidney | colon |
| C | 0.042 ± 0.006 | 0.017 ± 0.009 | 0.202 ± 0.048 | 0.026 ± 0.003 | 0.109 ± 0.020 | 0.056 ± 0.011 |
| Cd | 7.154 ± 0.724** | 9.070 ± 1.007** | 0.519 ± 0.020** | 0.078 ± 0.022 | 0.088 ± 0.011 | 0.055 ± 0.011 |
| L | 4.927 ± 0.232**## | 7.409 ± 0.672** | 0.504 ± 0.036** | 0.852 ± 0.069*# | 2.639 ± 0.360*# | 0.130 ± 0.038 |
| M | 2.886 ± 0.219**## | 7.324 ± 0.590** | 0.420 ± 0.072* | 3.413 ± 0.287**## | 8.183 ± 1.038**## | 1.069 ± 0.168**## |
| H | 1.452 ± 0.093## | 3.230 ± 0.553**## | 0.271 ± 0.024# | 5.013 ± 0.273**## | 10.377 ± 0.500**## | 2.731 ± 0.256**## |

Data were shown as mean ± SEM ($n = 6$). *$p < 0.05$, **$p < 0.01$ vs. control; #$p < 0.05$, ##$p < 0.01$ vs. Cd group.

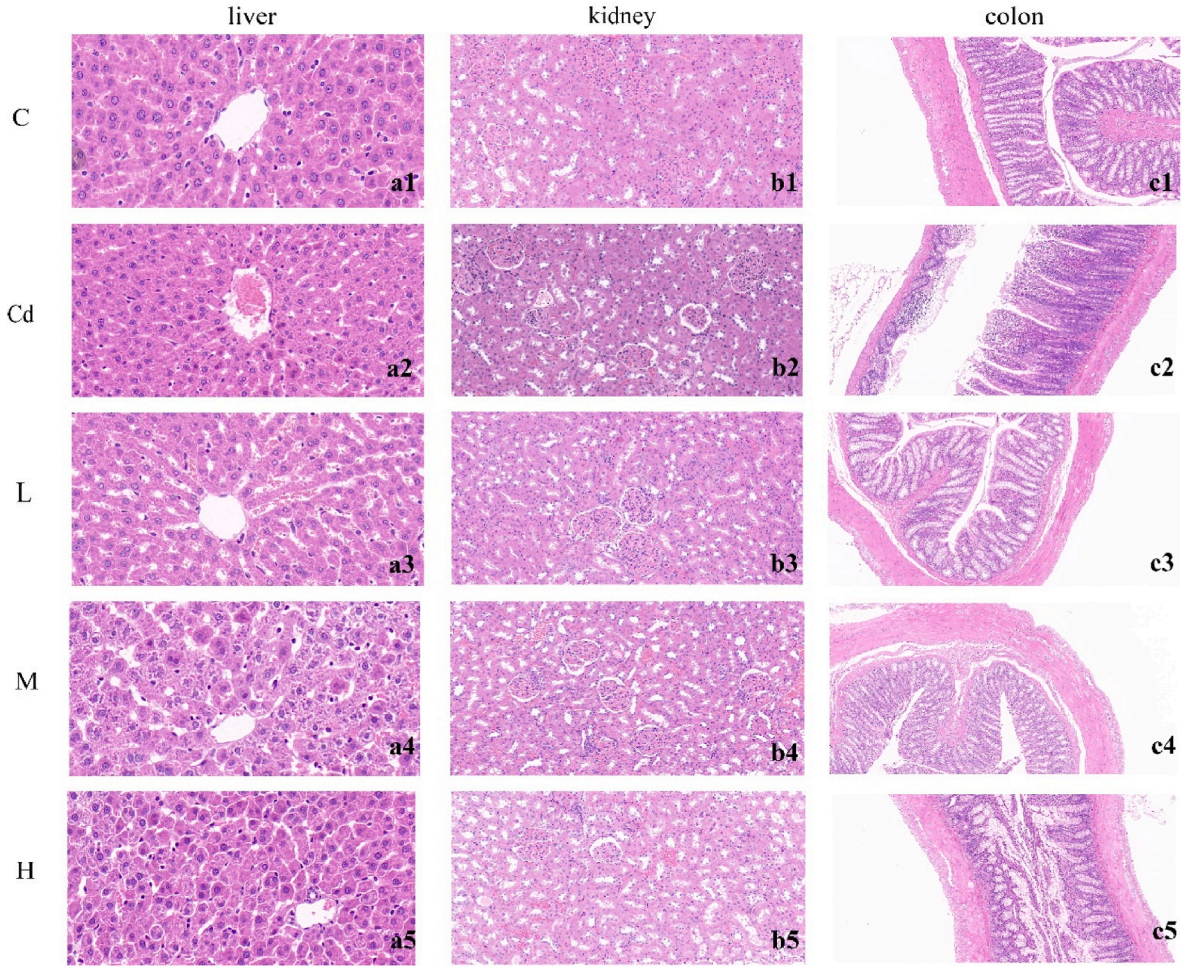


**Fig. 1.** Histology of liver, kidney, and colon sections. Samples were stained with Hematoxylin-Eosin and photomicrographs were taken using 40 × (liver), 20 × (kidney) and 10 × (colon) magnifications.

the L group (Fig. 1c3 and 1c4). In light of these results, our findings suggested that the low dosage of F might relief the histopathology damage mediated by Cd.

### 3.3. Low dosage of F reduces Cd-mediated hepatorenal function damage

Serum ALT and AST activities were evidently ($p < 0.05$ or $p < 0.01$) surged in the Cd group, which suggested the liver impairment (Fig. 2a, b and 2c). Compared to the Cd group, the ALT, AST, and AKP were reduced in the L group by 20.20%, 47.42%, and 10.99%, respectively. Compared to the C group, the levels of serum BUN, Cr and NAG were all significantly elevated after Cd exposure ($p < 0.01$) (Fig. 2d, e and 2f). However, all of them in the L group were significantly declined by 26.36% for BUN, 67.81% for Cr, and 36.68% for NAG, respectively ($p < 0.01$) (Fig. 2d, e and 2f). However, no obvious trend was observed in the M and H groups compared with Cd group in the liver and kidney. Totally, it could be concluded that there might be a protective effect of low F dosage on Cd-mediated hepatorenal function injuries in rats.

### 3.4. Low dosage of F inhibits Cd-mediated oxidative stress in liver and kidney

To elucidate the potential mechanism of F on Cd-induced oxidation stress, three indexes (MDA, SOD, and GSH-Px) (Fig. 3a, b, 3c, 3d, 3e and 3f) and genes (*Nrf2*, *NQO1,* and *HO1)* (Fig. 4a, b, 4c,4d, 4e and 4f) in the liver and kidney were evaluated. Relative to the C group, the MDA level was enhanced and SOD and GSH-Px activities were declined in the liver and kidney by Cd-treated. These data verified that Cd-treated might trigger hepatorenal oxidative stress. Relative to the Cd group, the level of MDA was decreased and the activities of SOD and GSH-Px were

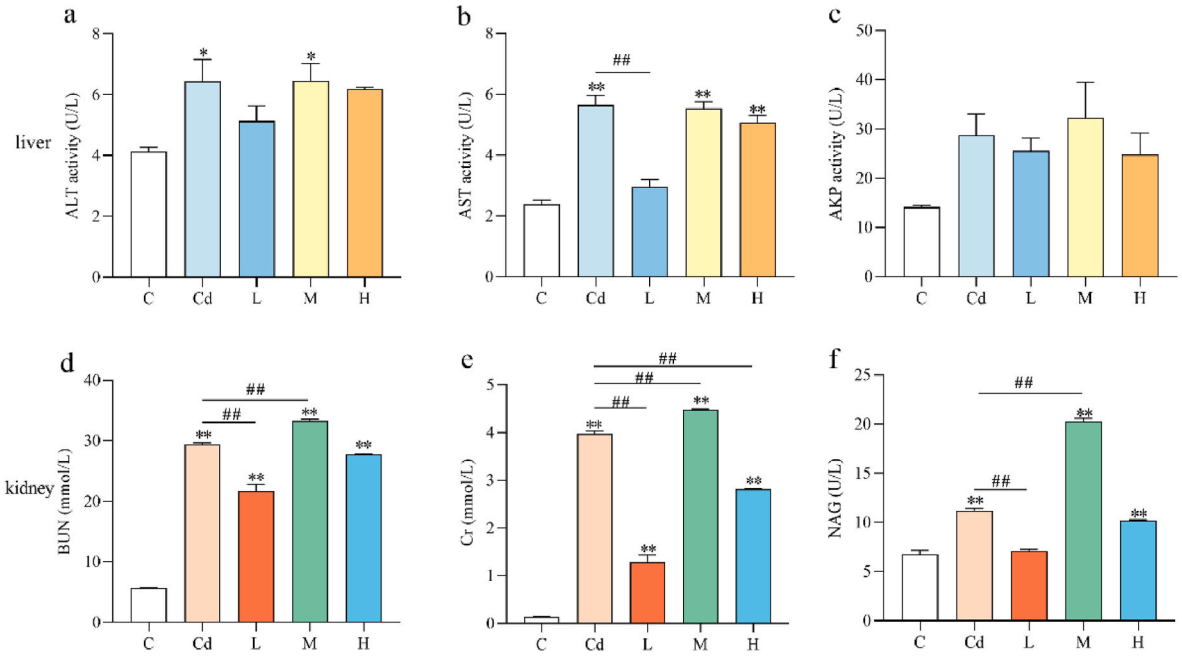


**Fig. 2.** Biochemical parameters. (a) ALT, (b) AST, (c)AKP, (d) BUN, (e) Cr, (f) NAG. Data were shown as mean ± SEM ($n = 3$). $^{*}p < 0.05$, $^{**}p < 0.01$ vs. control; $^{\#}p < 0.05$, $^{\#\#}p < 0.01$ vs. Cd group.

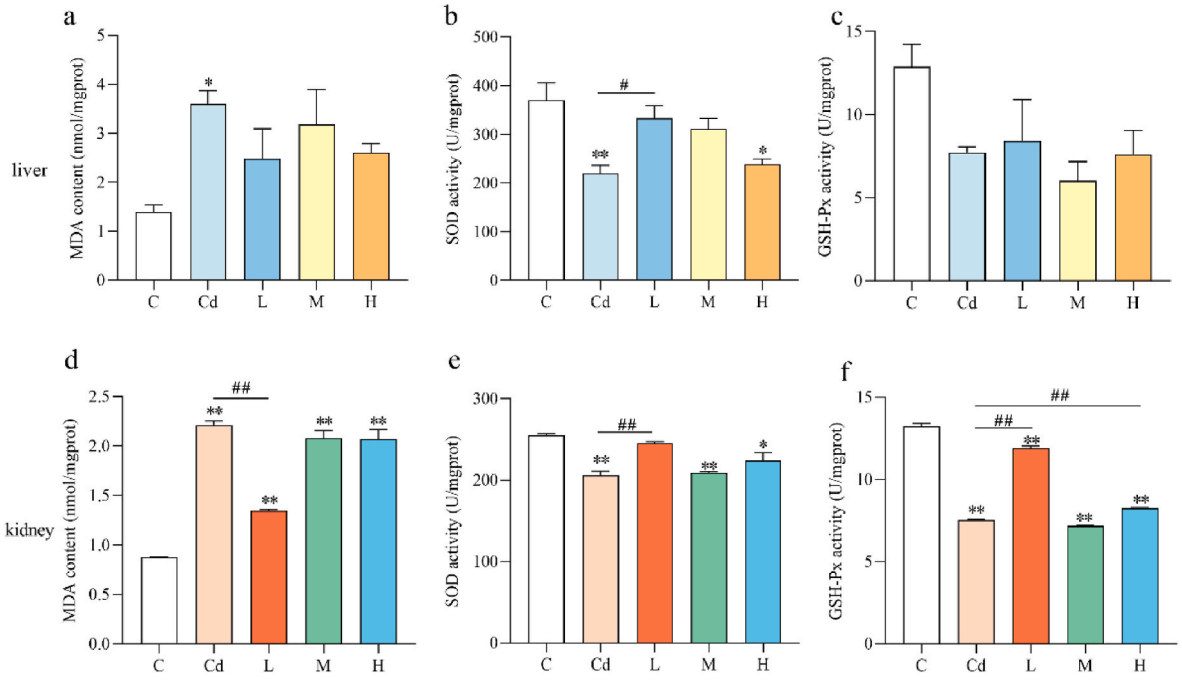


**Fig. 3.** The MDA, SOD and GSH-Px levels in the liver and kidney. (a–c) liver, (d–f) kidney. Data were shown as mean ± SEM ($n = 3$). $^{*}p < 0.05$, $^{**}p < 0.01$ vs. control; $^{\#}p < 0.05$, $^{\#\#}p < 0.01$ vs. Cd group.

elevated in the L group in the liver and kidney. However, these three indices in the M and H groups showed inconsistent trends compared to the Cd group.

Furthermore, compared with the C group, the mRNA expression levels of *NQO1*, *Nrf2* and *HQ1* in the liver and kidney were up-regulated in the Cd group (Fig. 4a, b, 4c, 4d, 4e and 4f). Compared to the Cd group, three indices in the L, M, and H groups were all declined in the kidney, while in the liver only in the L group showed an attenuation consistently. Collectively, we speculated that low dosage of F might be inclined to attenuate the Cd-induced oxidative stress.

### *3.5. F treatments showed a limited impact on gut microbial diversity alterations induced by Cd*

#### *3.5.1. Intestinal microbial richness and diversity*

Rarefaction curve was applied to measure if the present sequencing depth of every sample is enough to show the microbial diversity obtained in the community sample. With the increase of the effective sequence depth, the rarefaction curve of goods coverage first increased rapidly and then smoothed, indicating that the sample sequencing was saturated and covered all microbial species (Fig. 5a). A Venn diagram

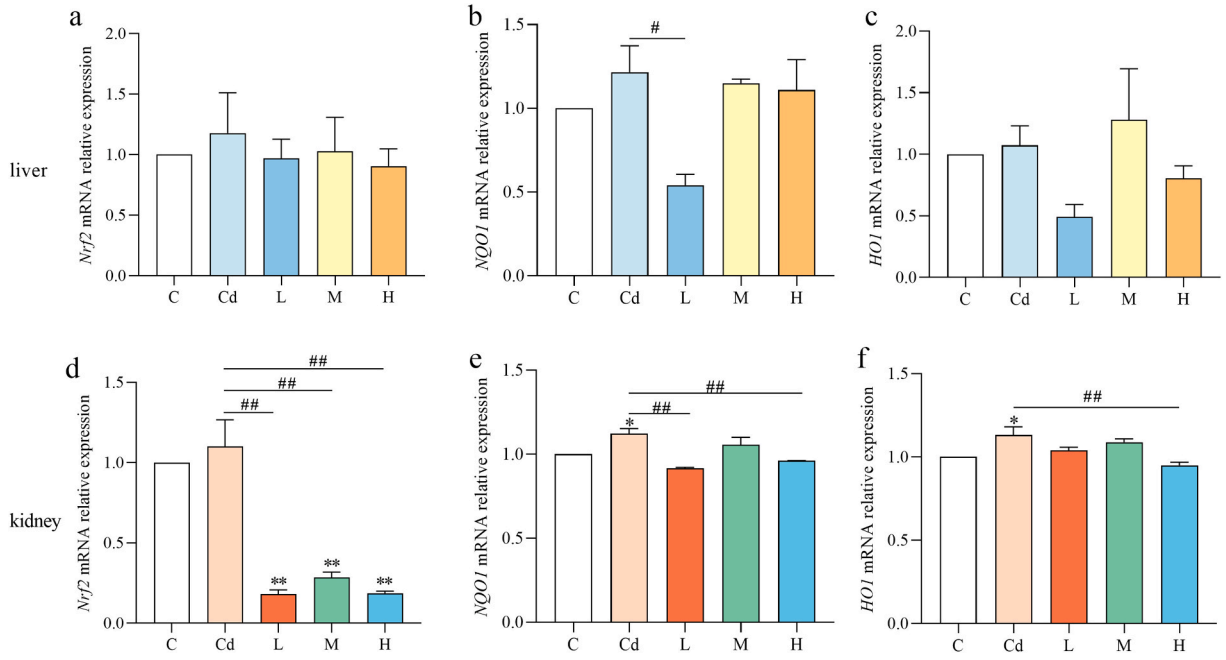


**Fig. 4.** The relative mRNA expression of *Nrf2*, *NQO1* and *HO1* in the liver and kidney. (a–c) liver, (d–f) kidney. Data were shown as mean ± SEM ($n = 3$). $^{*}p < 0.05$, $^{**}p < 0.01$ vs. control; $^{\#}p < 0.05$, $^{\#\#}p < 0.01$ vs. Cd group.

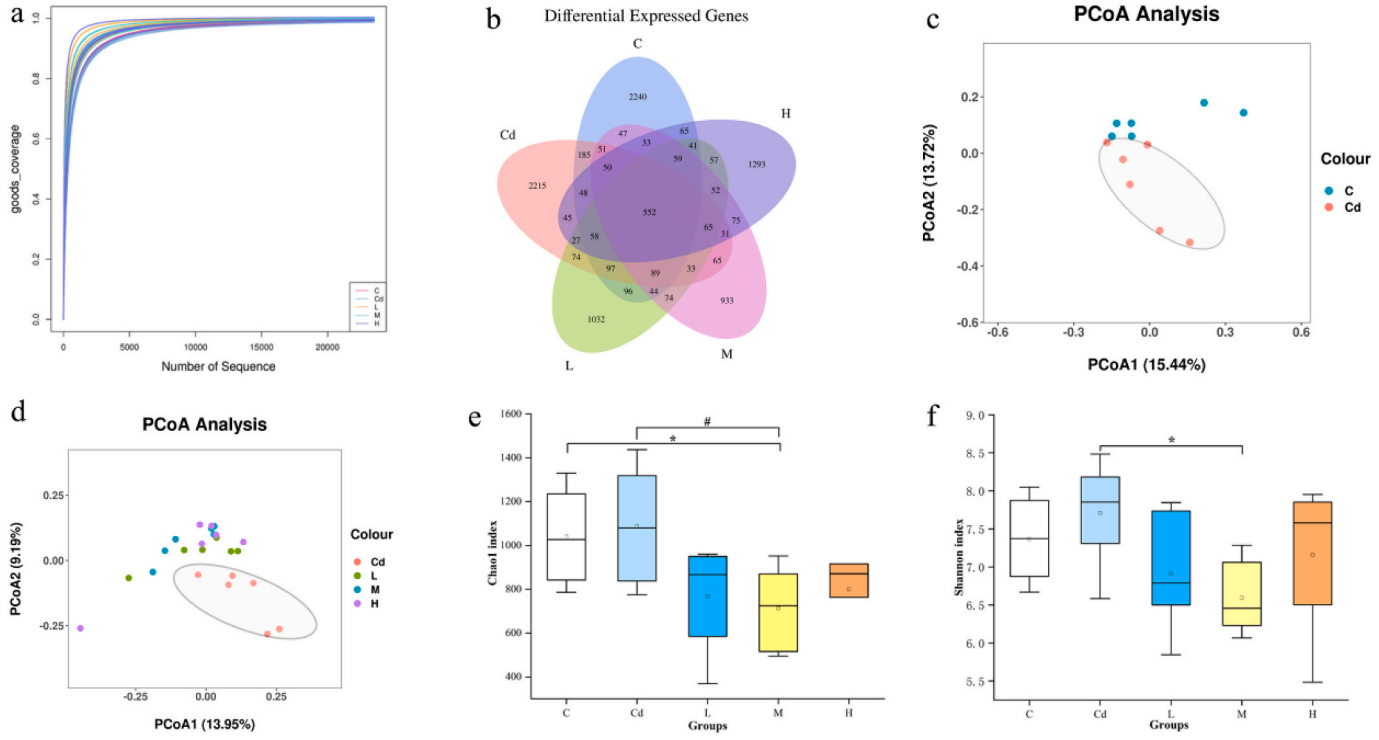


**Fig. 5.** The Cd and F exposure alters the alpha diversity and beta diversity analysis. (a) goods coverage curve; (b) the OTU in the different groups; (c–d) Principal Coordinate Analysis (PCoA); (e) Chao1 index; (f) Shannon index. $^{*}p < 0.05$ vs. control; $^{\#}p < 0.05$ vs. Cd group.

reflecting the overlaps was drawn to further observe the shared richness among exposed groups. It showed that means of 2240, 2215, 1032, 933, and 1293 OTUs were assigned to C, Cd, L, M, and H groups, and 552 OTUs coexisted in the five groups (Fig. 5b).

Alpha and beta diversities represent the bio-heterogeneity or overall diversity of a particular gut environmental community. The Chao 1 and Shannon indices (Fig. 5e and f) in the Cd group were greater than that in the C group. On the contrary, both of them were decreased in the L, M, and H groups in a comparison with the Cd group. However, no significant difference was examined among them with the exception of Cd versus M groups, indicating that the Cd and F exposure showed limited effects on the richness and diversity of intestinal community. Furthermore, the beta diversity estimated by PCoA was visually separated the exposed groups to better clarify the community difference at the OTU level. It demonstrated that the Cd exposure might alter the intestinal flora composition as the points were separated at a certain, and the F

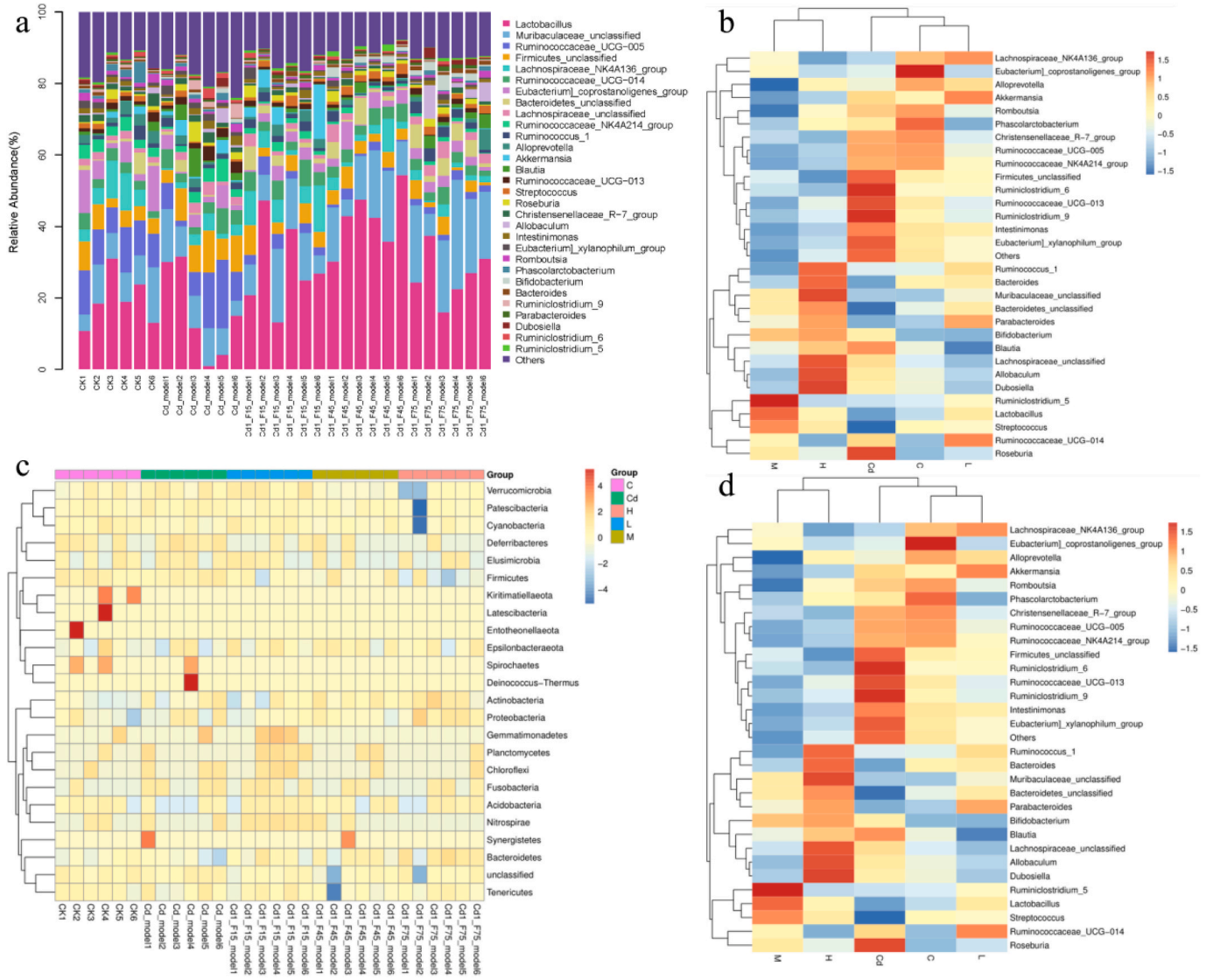


**Fig. 6.** The Cd and F exposure alters the gut microbiota composition. (a) Relative abundance of genus level; (b) Relative abundance of phylum level; (c) Dominant genera clustering heatmap; (d) Dominant phylum clustering heatmap.

exposure showed mild impact on Cd-induced alteration (Fig. 5c and d).

### 3.5.2. Intestinal microbiota composition

30 bacteria were identified and the abundance of dominant bacteria fluctuated among exposed groups (Fig. 6a and c). At the genus level, the *Lactobacillus, Ruminococcaceae_UCG-005, Lachnospiraceae_NK4A136_group*, and *Lachnospiraceae_NK4A136_group* were the dominant bacteria. Among them the relative abundances of *Lactobacillus* and *Lachnospiraceae_NK4A136_group* were obviously shifted. Relative to the C group, a decrease was reflected in the proportion of *Lactobacillus* and *Lachnospiraceae_NK4A136_group* of the Cd group. On the contrary, low dosage of F up-regulated the abundance of *Lactobacillus* from 15.56% (Cd group) to 28.73% (L group) and *Lachnospiraceae_NK4A136_group* from 2.40% (Cd group) to 6.63% (L group) (Fig. 6b), respectively. At the phylum level, the *Firmicutes/Bacteroidetes* (F/B) ratio of the Cd group was upper than that of the C group. By contrast, the F/B ratio in the *Lachnospiraceae_NK4A136_group* (3.70%) were declined compared to the Cd group (6.23%) (Fig. 6d). Moreover, the abundances of *Actinobacteria* and *Proteobacteria* in the Cd group were elevated compared to the C group. When compared to the Cd group, both of them were decreased after low supplementation of F. Totally, the results elucidated that microbial composition structure showed a certain response to the stress due to the Cd exposure and low F dosage might reverse the imbalance induced by Cd.

### 3.5.3. Differential analysis of intestinal microflora

The LEfSe analysis was estimated the variations of gut microbiota composition using cladogram and LDA score (above 4.0). Based on the results of both two approaches (Fig. 7b), *Ruminococcaceae_UCG_005* was enriched in the C group; *Clostridiales*, *Ruminococcaceae*, and *Firmicutes* were enriched in the Cd group; *Verrucomicrobiae*, *Akkermansiaceae*, and *Akkermansia* were main genera in the L group; *Bacilli*, *Lactobacillus*, and *Lactobacillaceae* were dominant in the M group; and *Bifidobacteriales*, *Bacteroidetes*, and *Actinobacteria* were dominant genera in the H group. It suggested that Cd exposure might adjust intestinal flora composition, while F supplements were possible to against Cd-induced alterations.

## 4. Discussion

Kinds of literatures have proved that co-exposure of Cd and F could generate adverse impacts on tissues and organs (Cinar et al., 2011; Melila et al., 2022). Early study has confirmed that low level of F could inhibit the decrease of vertebral bone mineral density mediated by Cd treatment (Chen et al., 2013). However, the research on the dose-effect

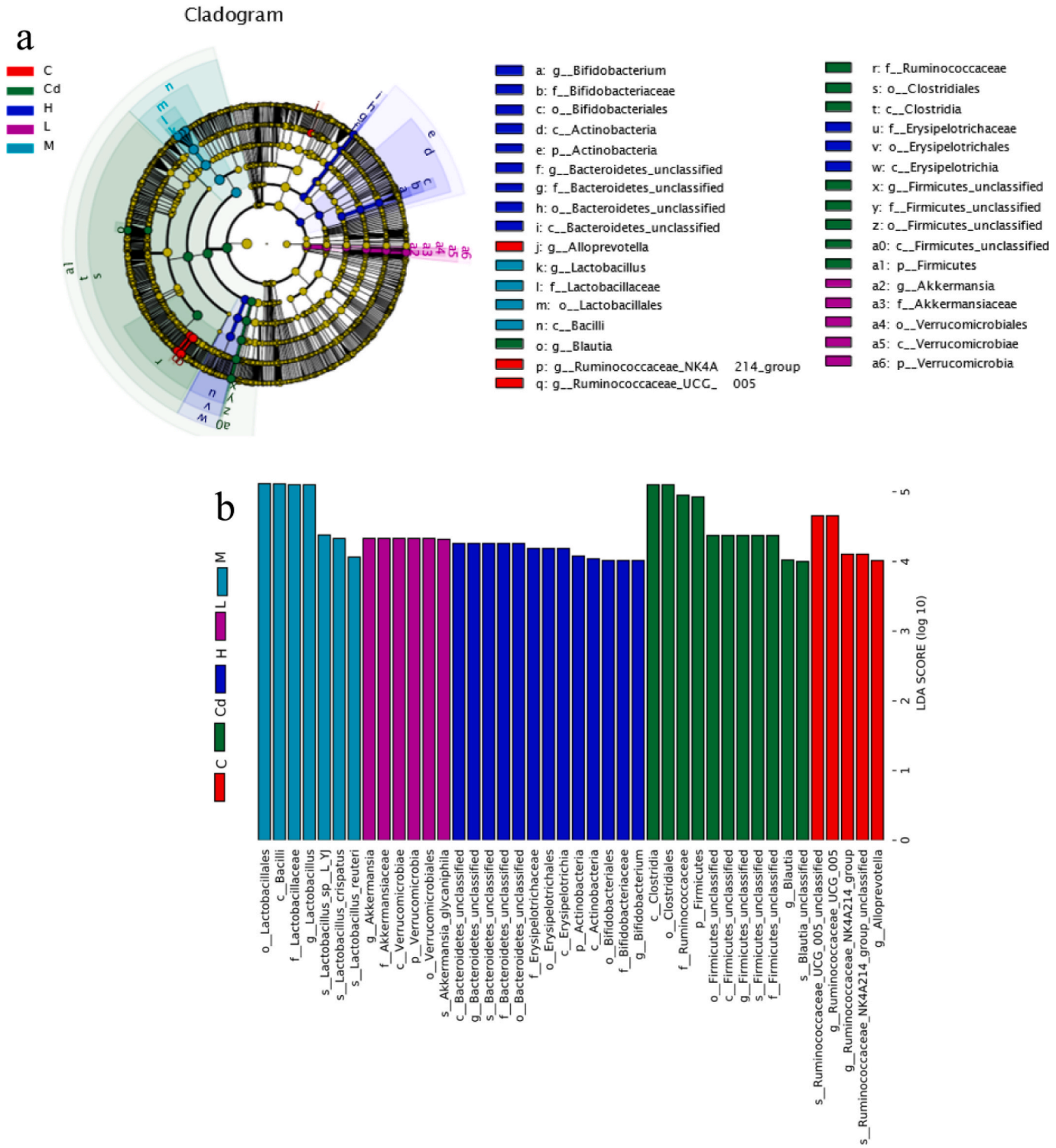


**Fig. 7.** The LEfSe analysis of discriminative taxa of gut microflora in rats. The cladogram (a) and linear discriminant analysis (LDA) score (b) were generated from LEfSe analysis. And only taxa meeting the LDA significance thresholds (>4.0) were shown.

of F on Cd-mediated biotoxicity is unprecedented. Here, we found that the low F dosage could suppress the Cd levels in organs, reverse the hepatorenal function damages and oxidative stress, and reshape the disorders of intestinal microbiota caused by Cd (Fig. 8).

The ease of F could bind to metals, and the metal-F complexes had poor solubility to facilitate excretion (Johnston and Strobel, 2020). In our study, the Cd levels in tissues were restrained by F supplement, indicating that F could inhibit the Cd accumulation in the organisms. Therefore, it might be a new strategy to reduce Cd toxicity by binding with F to discharge easily from the living organism. In addition, the distribution pattern of Cd in rats was in the order of kidney > liver > colon. It is well known that Cd is absorbed into the liver binding with metallothionein (MT) to form Cd-MT complexes, which reached the kidney on blood circulation (Fang et al., 2021). In turn, the Cd-MT complexes could be filtered by the glomerulus and reabsorbed by proximal tubule cells and rapidly degraded by lysosomal enzymes to

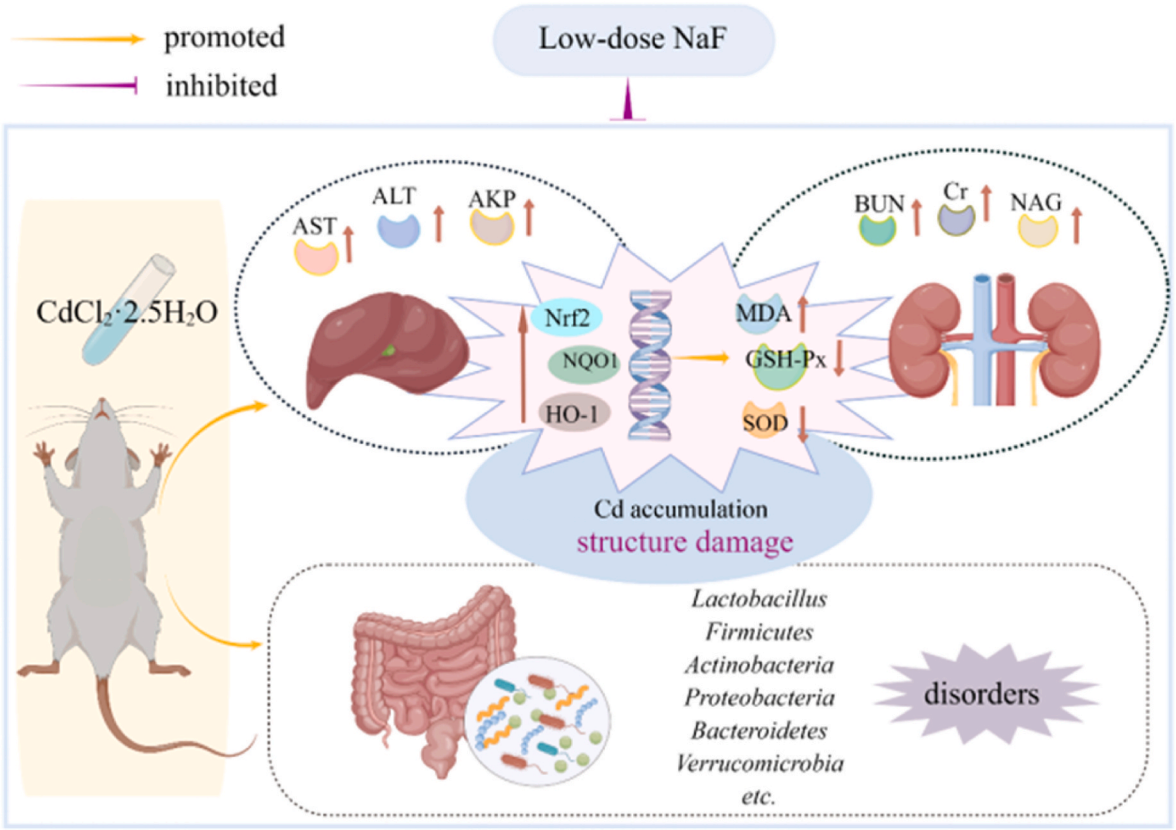


**Fig. 8.** The graphic showed the low dosage of F might attenuate the Cd toxicities in rats (By Figdraw ID: AIUIO31891).

release $Cd^{2+}$ ions, which might lead to the Cd enriching in the kidney (Liu et al., 2015; Yang and Shu, 2015). It could explain the higher levels of Cd in the kidney than that in the liver and gut.

Biochemical index is the basis for the diagnosis of diseases and the initial characteristics of toxicology estimation (Tian et al., 2021). AKP, AST and ALT mainly exist in liver cells, which are critical catalyst in the process of human metabolism and play roles when liver cells are impaired owing to poisoning and inflammation (Cinar et al., 2011). In this research, we observed that the low F treatment significantly reciprocated Cd-produced abnormalities in these serum biomarkers, indicating that protective effect of low dose of F could resist to Cd toxicity in liver. In addition, the determination of Cr, BUN, and NAG is one of the approaches to access kidney function (Pallio et al., 2019). The most important result was that the low F dosage could attenuate the renal function damage mediated by Cd via down-regulating of the levels of Cr, BUN, and NAG. Indeed, it is not objective to draw a conclusion whether there is an effect only through the detection of these apparent indicators. It is necessary to concentrate on the molecular level and other aspects to make the results more convincing and deeper.

Cd toxicity originates its prooxidative properties. Oxidative stress is one of the critical mechanisms by pollutants injuries living organisms (Valavanidis et al., 2006). Therefore, the elimination of oxidative stress might be a strategy to avoid Cd toxicity in organisms. SOD represents the activity of antioxidant enzymes, the level of MDA is a significant indicator showing the increase in lipid peroxidation rate, and GSH-Px is an antioxidant synthesized in cells with low molecular weight and can decrease the generation of free radicals (Gang et al., 2022; Park et al., 2021a; Pu et al., 2023; Renu et al., 2021). Regardless of liver or kidney, scientific studies evidenced that Cd exposure could occur oxidative stress through down-regulating the activities of SOD and GSH-Px, and up-regulating the concentration of MDA (Kostecka-Sochon et al., 2018; Li et al., 2021; Park et al., 2021b), which is correspond to our results. However, the MDA content was decreased and the activities of SOD and GSH-Px were increased with the low supplementation of F, suggesting that it might adjust the disorder of anti-oxidant system. *Nrf2*, distributes in the cytoplasm and combined with *Keap 1*, is a transcription factor that enhances protective genes in response to oxidative stress (Wu et al., 2012). Thus far, a great deal of research endorsed the point that Cd exposure activated mRNA expression *of Nrf2* (Xue et al., 2021; Zheng et al., 2016). At the molecular level, Chen et al. (2019) demonstrated that Cd suppressed the activation of the *Nrf2* signaling pathway through remarkably up-regulating the mRNA expressions of *Nrf2*, as well as its downstream factor *HO1* and *NQO1* in the kidney. Similarly, our study verified that Cd exposure enhanced the expression of *Nrf2*, *HO1* and *NQO1* in the liver and kidney. By contrast, the expression of these genes was inhibited significantly after the low F application, indicating the intervention of F in the *Nrf2* pathway.

The intestinal microbiota, a complicated community of microbes in the rat gut, is crucial for host health. Our experiment took the colon tissue into consideration since it is the location of one of the most diverse human microbiomes (Nagpal et al., 2014). The fundamental probiotic effects of *Lactobacillus* against pathogens present in the gut tract and have been proven to inhibit the growth of urogenital pathogens such as *G. vaginalis* and *P. aeruginosa* (Chee et al., 2020). In our study, Cd exposure perturbed the composition of gut microbiota in rats, especially decreasing the abundance of *Lactobacillus*. However, low level of F could promote the growth of *Lactobacillus* by Cd-mediated. In addition, Chen et al. suggested the F in a suitable dosage is beneficial and expected to serve as a food additive in suitable dosage to improve human health through modulation of the gut microbiota (Chen et al., 2021a). Therefore, it provides an evidence that low F exposure has the potential to inhibit the perturbation of intestinal composition mediated by Cd. However, the relationship between contaminants and gut microbiota was complicated. In our research, we only found that F could affect the alterations of gut microbiota composition, while the potential mechanism is still scarce. Therefore, more studies should be implemented to

evidence these results in the future.

## 5. Conclusion

The present study has inferred that low dosage of F has the potential to attenuate Cd-induced biotoxicity. Specifically, low F treatment could inhibit the accumulation of Cd, enhance the levels of serum biomarkers, promote the activities of antioxidant enzymes, and modulate gut microbiota. It is suggested that low F dosage might be used as a supplement to minimize the adverse effect of Cd in rats. However, the effects of M and H dosages of F on the Cd-induced toxicity were unobvious in our study, which showed disparate and even opposite. Therefore, it is expected to design more detailed concentration gradient at the molecular level to further make clear the mechanism of the effects of F on Cd-mediated toxicity in the future study.

## Credit authors statement

**Qinghai Zhang**: Conceptualization, methodology, validation, investigation, writing – original draft, Writing – review & editing, project administration, supervision. **Dashuan Li and Chaolian Yang**: Conceptualization, methodology, investigation, validation. **Xiaomei Xu, Shanghang Li and Guofei Luo**: methodology, conceptualization. **Cheng Zhang and Zelan Wang**: Resources, investigation, supervision. **Dali Sun and Jianzhong Cheng:** Formal analysis.

## Ethics statement

The animal study was reviewed and approved by the Ethics Committee of Guizhou Medical University.

## Declaration of competing interest

The authors declare that they have no known competing financial interests or personal relationships that could have appeared to influence the work reported in this paper.

## Data availability

Data will be made available on request.

## Acknowledgment

The authors would like to acknowledge the financial support from the National Natural Science Foundation of China grant number [42167054], the Open Foundation for Key Laboratory of Environmental Pollution Monitoring and Disease Control, Ministry of Education ([2022] 441), and the Engineering Research Center of Higher Education Institutions in Guizhou province, China grant number [KY2020014, KY 2021 008].

## Appendix A. Supplementary data

Supplementary data to this article can be found online at https://doi.org/10.1016/j.envpol.2023.121375.

## References

Alhusaini, A., Faddaa, L., Ali, H.M., Hassan, I., El Orabi, N.F., Bassiouni, Y., 2018. Amelioration of the protein expression of Cox2, NFkappaB, and STAT-3 by some antioxidants in the liver of Sodium fluoride-intoxicated rats. Dose Response 16, 1559325818800153. https://doi.org/10.1177/1559325818800153.

Ba, Q., Li, M., Chen, P., Huang, C., Duan, X., Lu, L., Li, J., Chu, R., Xie, D., Song, H., Wu, Y., Ying, H., Jia, X., Wang, H., 2017. Sex-dependent effects of cadmium exposure in early life on gut microbiota and fat accumulation in mice. Environ. Health Perspect. 125, 437–446. https://doi.org/10.1289/EHP360.

Bhardwaj, J.K., Panchal, H., Saraf, P., 2021. Cadmium as a testicular toxicant: a Review. J. Appl. Toxicol. 41, 105–117. https://doi.org/10.1002/jat.4055.

Chee, W.J.Y., Chew, S.Y., Than, L.T.L., 2020. Vaginal microbiota and the potential of Lactobacillus derivatives in maintaining vaginal health. Microb. Cell Factories 19, 203. https://doi.org/10.1186/s12934-020-01464-4.

Chen, G., Hu, P., Xu, Z., Peng, C., Wang, Y., Wan, X., Cai, H., 2021a. The beneficial or detrimental fluoride to gut microbiota depends on its dosages. Ecotoxicol. Environ. Saf. 209 https://doi.org/10.1016/j.ecoenv.2020.111732.

Chen, G., Hu, P., Xu, Z., Peng, C., Wang, Y., Wan, X., Cai, H., 2021b. The beneficial or detrimental fluoride to gut microbiota depends on its dosages. Ecotoxicol. Environ. Saf. 209, 111732 https://doi.org/10.1016/j.ecoenv.2020.111732.

Chen, X., Qin, B., Li, X., Jin, T., Zhu, G., Zhou, W., Wang, Z., 2013. Effects of fluoride and cadmium co-exposure on bone in male rats. Biol. Trace Elem. Res. 154, 396–402. https://doi.org/10.1007/s12011-013-9750-4.

Chen, Z.J., Chen, J.X., Wu, L.K., Li, B.Y., Tian, Y.F., Xian, M., Huang, Z.P., Yu, R.A., 2019. Induction of endoplasmic reticulum stress by cadmium and its regulation on Nrf2 signaling pathway in kidneys of rats. Biomed. Environ. Sci. 32, 1–10. https://doi.org/10.3967/bes2019.001.

Cinar, M., Yigit, A.A., Yalcinkaya, I., Oruc, E., Duru, O., Arslan, M., 2011. Cadmium induced changes on growth performance, some biochemical parameters and tissue in broilers: effects of vitamin C and vitamin E. Asian J. Anim. Vet. Adv. 6, 923–934. https://doi.org/10.3923/ajava.2011.923.934.

Duan, Y., Wang, Y., Huang, J., Li, H., Dong, H., Zhang, J., 2021. Toxic effects of cadmium and lead exposure on intestinal histology, oxidative stress response, and microbial community of Pacific white shrimp Litopenaeus vannamei. Mar. Pollut. Bull. 167, 112220 https://doi.org/10.1016/j.marpolbul.2021.112220.

Fan, R.F., Li, Z.F., Zhang, D., Wang, Z.Y., 2020. Involvement of Nrf2 and mitochondrial apoptotic signaling in trehalose protection against cadmium-induced kidney injury. Metallomics 12, 2098–2107. https://doi.org/10.1039/d0mt00213e.

Fang, J., Xie, S., Chen, Z., Wang, F., Chen, K., Zuo, Z., Cui, H., Guo, H., Ouyang, P., Chen, Z., Huang, C., Liu, W., Geng, Y., 2021. Protective effect of vitamin E on cadmium-induced renal oxidative damage and apoptosis in rats. Biol. Trace Elem. Res. 199, 4675–4687. https://doi.org/10.1007/s12011-021-02606-4.

Gang, H., Junrong, L., Huiling, G., Xueru, W., Zhisheng, H., Wenjing, P., Xuesheng, C., Caiying, Z., 2022. Molybdenum and cadmium co-exposure promotes M1 macrophage polarization through oxidative stress-mediated inflammatory response and induces pulmonary fibrosis in Shaoxing ducks (Anas platyrhyncha). Environ. Toxicol. 37.

Gong, Z.G., Zhao, Y., Wang, Z.Y., Fan, R.F., Liu, Z.P., Wang, L., 2022. Epigenetic regulator BRD4 is involved in cadmium-induced acute kidney injury via contributing to lysosomal dysfunction, autophagy blockade and oxidative stress. J. Hazard Mater. 423, 127110 https://doi.org/10.1016/j.jhazmat.2021.127110.

Han, Y., Yu, Y., Liang, C., Shi, Y., Zhu, Y., Zheng, H., Wang, J., Zhang, J., 2019. Fluoride-induced unrestored arrest during haploid period of spermatogenesis via the regulation of DDX25 in rats. Environ. Pollut. 253, 538–551. https://doi.org/10.1016/j.envpol.2019.06.107.

Johnston, N.R., Strobel, S.A., 2020. Principles of fluoride toxicity and the cellular response: a review. Arch. Toxicol. 94, 1051–1069. https://doi.org/10.1007/s00204-020-02687-5.

Kostecka-Sochon, P., Onopiuk, B.M., Dabrowska, E., 2018. Protective effect of increased zinc supply against oxidative damage of sublingual gland in chronic exposure to cadmium: experimental study on rats. Oxid. Med. Cell. Longev., 3732842 https://doi.org/10.1155/2018/3732842, 2018.

Li, F., Liao, S., Zhao, Y., Li, X., Wang, Z., Liao, C., Sun, D., Zhang, Q., Lu, Q., 2023. Soil exposure is the major fluoride exposure pathways for residents from the high-fluoride karst region in Southwest China. Chemosphere 310, 136831. https://doi.org/10.1016/j.chemosphere.2022.136831.

Li, X., Zhou, L., Zhang, C., Li, D., Wang, Z., Sun, D., Liao, C., Zhang, Q., 2022. Spatial distribution and risk assessment of fluorine and cadmium in rice, corn, and wheat grains in most karst regions of Guizhou province, China. Front. Nutr. 9, 1014147 https://doi.org/10.3389/fnut.2022.1014147.

Li, Y., Wang, S., Nan, Z., Zang, F., Sun, H., Zhang, Q., Huang, W., Bao, L., 2019. Accumulation, fractionation and health risk assessment of fluoride and heavy metals in soil-crop systems in northwest China. Sci. Total Environ. 663, 307–314. https://doi.org/10.1016/j.scitotenv.2019.01.257.

Li, Z., Ali Shah, S.W., Zhou, Q., Yin, X., Teng, X., 2021. The contributions of miR-25-3p, oxidative stress, and heat shock protein in a complex mechanism of autophagy caused by pollutant cadmium in common carp (Cyprinus carpio L.) hepatopancreas. Environ. Pollut. 287, 117554 https://doi.org/10.1016/j.envpol.2021.117554.

Liu, J., Wang, H.W., Lin, L., Miao, C.Y., Zhang, Y., Zhou, B.H., 2019. Intestinal barrier damage involved in intestinal microflora changes in fluoride-induced mice. Chemosphere 234, 409–418. https://doi.org/10.1016/j.chemosphere.2019.06.080.

Liu, K., Chi, S., Liu, H., Dong, X., Yang, Q., Zhang, S., Tan, B., 2015. Toxic effects of two sources of dietborne cadmium on the juvenile cobia, Rachycentron canadum L. and tissue-specific accumulation of related minerals. Aquat. Toxicol. 165, 120–128. https://doi.org/10.1016/j.aquatox.2015.05.013.

Melila, M., Rajaram, R., Ganeshkumar, A., Kpemissi, M., Pakoussi, T., Agbere, S., Lazar, I. M., Lazar, G., Amouzou, K., Paray, B.A., Gulnaz, A., 2022. Assessment of renal and hepatic dysfunction by co-exposure to toxic metals (Cd, Pb) and fluoride in people living nearby an industrial zone. J. Trace Elem. Med. Biol. 69, 126890 https://doi.org/10.1016/j.jtemb.2021.126890.

Milad, A.-N., Ebrahim, M., Mohammad, S., Nematollah, A., Talebpour, A.F., Fatemeh, S., 2020. Co-exposure to non-toxic levels of cadmium and fluoride induces hepatotoxicity in rats via triggering mitochondrial oxidative damage, apoptosis, and NF-kB pathways. Environ. Sci. Pollut. Res. Int. 27.

Nagpal, R., Yadav, H., Marotta, F., 2014. Gut microbiota: the next-gen frontier in preventive and therapeutic medicine? Front. Med. 1, 15. https://doi.org/10.3389/fmed.2014.00015.

Nair, A.R., Lee, W.K., Smeets, K., Swennen, Q., Sanchez, A., Thevenod, F., Cuypers, A., 2015. Glutathione and mitochondria determine acute defense responses and adaptive processes in cadmium-induced oxidative stress and toxicity of the kidney. Arch. Toxicol. 89, 2273–2289. https://doi.org/10.1007/s00204-014-1401-9.

Pallio, G., Micali, A., Benvenga, S., Antonelli, A., Marini, H.R., Puzzolo, D., Macaione, V., Trichilo, V., Santoro, G., Irrera, N., Squadrito, F., Altavilla, D., Minutoli, L., 2019. Myo-inositol in the protection from cadmium-induced toxicity in mice kidney: an emerging nutraceutical challenge. Food Chem. Toxicol. 132, 110675 https://doi.org/10.1016/j.fct.2019.110675.

Park, E., Kim, J., Kim, B., Park, E.Y., 2021a. Association between environmental exposure to cadmium and risk of suspected non-alcoholic fatty liver disease. Chemosphere 266, 128947. https://doi.org/10.1016/j.chemosphere.2020.128947.

Park, J.H., Lee, B.M., Kim, H.S., 2021b. Potential protective roles of curcumin against cadmium-induced toxicity and oxidative stress. J. Toxicol. Environ. Health B Crit. Rev. 24, 95–118. https://doi.org/10.1080/10937404.2020.1860842.

Pu, W., Chu, X., Guo, H., Huang, G., Cui, T., Huang, B., Dai, X., Zhang, C., 2023. The activated ATM/AMPK/mTOR axis promotes autophagy in response to oxidative stress-mediated DNA damage co-induced by molybdenum and cadmium in duck testes. Environ. Pollut. 316, 120574 https://doi.org/10.1016/j.envpol.2022.120574.

Quadri, J.A., Sarwar, S., Sinha, A., Kalaivani, M., Dinda, A.K., Bagga, A., Roy, T.S., Das, T.K., Shariff, A., 2018. Fluoride-associated ultrastructural changes and apoptosis in human renal tubule: a pilot study. Hum. Exp. Toxicol. 37, 1199–1206. https://doi.org/10.1177/0960327118755257.

Renu, K., Chakraborty, R., Myakala, H., Koti, R., Famurewa, A.C., Madhyastha, H., Vellingiri, B., George, A., Valsala Gopalakrishnan, A., 2021. Molecular mechanism of heavy metals (lead, chromium, arsenic, mercury, nickel and cadmium) - induced hepatotoxicity - a review. Chemosphere 271, 129735. https://doi.org/10.1016/j.chemosphere.2021.129735.

Shi, X., Xu, T., Cui, W., Qi, X., Xu, S., 2023. Combined negative effects of microplastics and plasticizer DEHP: the increased release of Nets delays wound healing in mice. Sci. Total Environ. 862, 160861 https://doi.org/10.1016/j.scitotenv.2022.160861.

Shi, X., Zhu, W., Chen, T., Cui, W., Li, X., Xu, S., 2022. Paraquat induces apoptosis, programmed necrosis, and immune dysfunction in CIK cells via the PTEN/PI3K/AKT axis. Fish Shellfish Immunol. 130, 309–316. https://doi.org/10.1016/j.fsi.2022.09.024.

Tian, X., Ding, Y., Kong, Y., Wang, G., Wang, S., Cheng, D., 2021. Purslane (Portulacae oleracea L.) attenuates cadmium-induced hepatorenal and colonic damage in mice: role of chelation, antioxidant and intestinal microecological regulation. Phytomedicine 92, 153716. https://doi.org/10.1016/j.phymed.2021.153716.

Tian, X., Feng, J., Dong, N., Lyu, Y., Wei, C., Li, B., Ma, Y., Xie, J., Qiu, Y., Song, G., Ren, X., Yan, X., 2019. Subchronic exposure to arsenite and fluoride from gestation to puberty induces oxidative stress and disrupts ultrastructure in the kidneys of rat offspring. Sci. Total Environ. 686, 1229–1237. https://doi.org/10.1016/j.scitotenv.2019.04.409.

Valavanidis, A., Vlahogianni, T., Dassenakis, M., Scoullos, M., 2006. Molecular biomarkers of oxidative stress in aquatic organisms in relation to toxic environmental pollutants. Ecotoxicol. Environ. Saf. 64, 178–189. https://doi.org/10.1016/j.ecoenv.2005.03.013.

Wang, H., Wang, A., Wang, X., Zeng, X., Xing, H., 2022. AMPK/PPAR-γ/NF-κB axis participates in ROS-mediated apoptosis and autophagy caused by cadmium in pig liver. Environ. Pollut. 294, 118659 https://doi.org/10.1016/j.envpol.2021.118659.

Wang, J., Yang, J., Cheng, X., Xiao, R., Zhao, Y., Xu, H., Zhu, Y., Yan, Z., Ommati, M.M., Manthari, R.K., Wang, J., 2019. Calcium alleviates fluoride-induced bone damage by inhibiting endoplasmic reticulum stress and mitochondrial dysfunction. J. Agric. Food Chem. 67, 10832–10843. https://doi.org/10.1021/acs.jafc.9b04295.

Wang, N., Guo, Z., Zhang, Y., Zhang, P., Liu, J., Cheng, Y., Zhang, L., Li, Y., 2020. Effect on intestinal microbiota, bioaccumulation, and oxidative stress of Carassius auratus gibelio under waterborne cadmium exposure. Fish Physiol. Biochem. 46, 2299–2309. https://doi.org/10.1007/s10695-020-00870-0.

Wang, R., Sang, P., Guo, Y., Jin, P., Cheng, Y., Yu, H., Xie, Y., Yao, W., Qian, H., 2023. Cadmium in food: source, distribution and removal. Food Chem. 405, 134666 https://doi.org/10.1016/j.foodchem.2022.134666.

Wu, K.C., Liu, J.J., Klaassen, C.D., 2012. Nrf2 activation prevents cadmium-induced acute liver injury. Toxicol. Appl. Pharmacol. 263, 14–20. https://doi.org/10.1016/j.taap.2012.05.017.

Xu, S., Xiaojing, L., Xinyue, S., Wei, C., Honggui, L., Shiwen, X., 2021. Pig lung fibrosis is active in the subacute CdCl(2) exposure model and exerts cumulative toxicity through the M1/M2 imbalance. Ecotoxicol. Environ. Saf. 225, 112757 https://doi.org/10.1016/j.ecoenv.2021.112757.

Xu, T., Liu, Q., Chen, D., Liu, Y., 2022. Atrazine exposure induces necroptosis through the P450/ROS pathway and causes inflammation in the gill of common carp (Cyprinus carpioL.). Fish Shellfish Immunol. 131, 809–816. https://doi.org/10.1016/j.fsi.2022.10.022.

Xue, H., Cao, H., Xing, C., Feng, J., Zhang, L., Zhang, C., Hu, G., Yang, F., 2021. Selenium triggers Nrf2-AMPK crosstalk to alleviate cadmium-induced autophagy in rabbit cerebrum. Toxicology 459, 152855. https://doi.org/10.1016/j.tox.2021.152855.

Yang, H., Shu, Y., 2015. Cadmium transporters in the kidney and cadmium-induced nephrotoxicity. Int. J. Mol. Sci. 16, 1484–1494. https://doi.org/10.3390/ijms16011484.

Yu, X., Xia, L., Zhang, S., Zhou, G., Li, Y., Liu, H., Hou, C., Zhao, Q., Dong, L., Cui, Y., Zeng, Q., Wang, A., Liu, L., 2021. Fluoride exposure and children's intelligence: gene-environment interaction based on SNP-set, gene and pathway analysis, using a case-control design based on a cross-sectional study. Environ. Int. 155, 106681 https://doi.org/10.1016/j.envint.2021.106681.

Yu, Y.Q., Yang, J.Y., 2020. Health risk assessment of fluorine in fertilizers from a fluorine contaminated region based on the oral bioaccessibility determined by Biomimetic Whole Digestion-Plasma in-vitro Method (BWDPM). J. Hazard Mater. 383, 121124 https://doi.org/10.1016/j.jhazmat.2019.121124.

Zhang, C., Li, X.N., Xiang, L.R., Qin, L., Lin, J., Li, J.L., 2017. Atrazine triggers hepatic oxidative stress and apoptosis in quails (Coturnix C. coturnix) via blocking Nrf2-mediated defense response. Ecotoxicol. Environ. Saf. 137, 49–56. https://doi.org/10.1016/j.ecoenv.2016.11.016.

Zhang, J., Song, J., Zhang, J., Chen, X., Zhou, M., Cheng, G., Xie, X., 2013. Combined effects of fluoride and cadmium on liver and kidney function in male rats. Biol. Trace Elem. Res. 155, 396–402. https://doi.org/10.1007/s12011-013-9807-4.

Zheng, J.L., Yuan, S.S., Wu, C.W., Li, W.Y., 2016. Chronic waterborne zinc and cadmium exposures induced different responses towards oxidative stress in the liver of zebrafish. Aquat. Toxicol. 177, 261–268. https://doi.org/10.1016/j.aquatox.2016.06.001.